THE ESTIMATION OF THE STABILITY AND CONTROL CHARACTERISTICS OF A CANARD CONFIGURED COMBAT AIRCRAFT HAVING A FORWARD SWEPT WING

ICAS-86-5.5.1

M. V. Cook and F. Heydari
College of Aeronautics
Cranfield Institute of Technology
Cranfield, Bedford

ABSTRACT

A programme of research has been undertaken in which the principal objective has been to investigate the stability and control characteristics of a generalised canard configured combat aircraft having a forward swept wing. A detailed design study was undertaken to produce an aircraft configured for optimum aerodynamic performance whilst retaining defined, but adjustable, stability margins. A dynamically scaled wind tunnel model with active controls was built and flown on a purpose built test rig in a low speed wind tunnel. Model motion was limited by the test rig to the four degrees of freedom in roll, pitch, yaw and heave. Tests were carried out in which the control input and model response time histories were recorded and stored in digital data files for subsequent analysis. A parameter estimation program using an extended Kalman filter algorithm was written and developed to analyse the response data and from which the output was a set of estimated stability derivatives. This work has produced some very credible results which compare favourably with similar results estimated by less sophisticated means. In this paper the development of the Kalman filter algorithm and its application to the experimental facility is described and presented with some typical results.

INTRODUCTION

The work described in this paper represents a small but significant contribution to a broader programme of research in which the principal objective has been to investigate the stability and control characteristics of a canard configured combat aircraft having a forward swept wing (FSW). A specification for such an aircraft was written and a design study was undertaken to produce a reasonably representative single engine configuration having an optimised aerodynamic performance. Attempts to estimate the stability and control characteristics of the configuration theoretically were made but the confidence in the results was low, largely due to the inadequacy of available information and estimation techniques. Consequently, subsequent efforts were concentrated on wind tunnel tests involving a one fourteenth scale model of the aircraft mounted in a dynamic test rig. The model was dynamically scaled for operation in a limited subsonic flight envelope as determined by the maximum speed of the tunnel facility used.

Once the model and experimental facility were fully developed and calibrated it was possible to fly the model in the wind tunnel with a limited number of degrees of freedom. The model could be disturbed from equilibrium by the application of precise control surface inputs and the response recorded. Digital records of the input and output time histories were then used by the parameter identification computer programs to estimate the aerodynamic stability and control derivatives for the aircraft model. The parameter identification software was developed from first principles and utilises a standard Kalman filter estimator tailored specifically to this application. Great care was exercised in the development of the experimental facility and parameter identification software to ensure that consistent results could be obtained. With the experimental facility established, estimation of the model stability characteristics was carried out for various flight conditions and stability margins, including unstable configurations, and with the inclusion of various autostabilisation and autopilot feedback loops. In general the results obtained were of very good quality and, despite the limitation of scale and of the simulated flight envelope, the stability derivative estimates obtained were considered to be quite representative. A detailed report on this work is included in the thesis by Heydari[7].

In the following sections the background to the parameter estimation process is discussed together with a brief description of its application to the experimental facility. This is followed by a description of the validation techniques and concludes with some typical results which serve to illustrate the success of the exercise and the expected characteristics of a FSW fighter aircraft configuration.

THE FSW AIRCRAFT DESIGN

The requirement for the aircraft was that it should be a canard configured combat aircraft having proportions representative of that class of aircraft whilst simultaneously having an optimised aerodynamic performance. Although initially to be stable, unstable developments were not ruled out. The aircraft was represented by a number of structural, system and other components each having defined mass distribution and volumetric properties. Additionally, a number of theoretical models describing the configuration aerodynamics were developed. All of this basic information was incorporated into a specially written computer program which iterated the leading configuration dimensions in order to optimise a number of prescribed criteria. These criteria could be chosen by the operator and included, mass, aspect ratio, stability margin and maximum lift to drag ratio. As this software was developed to accommodate improved aerodynamic models so the configurations it produced began to resemble realisable aircraft. Later developments of the software also attempted to estimate aerodynamic stability derivatives but with very limited success. Early developments of this work are reported by Cook and O'Riordan[4] and by O'Riordan[5] whereas later developments leading to the current design are reported by Heydari[7], and summarised by Heydari and Cook[6].

The notional FSW aircraft design produced by this technique has a total mass of 9100 kg and a wing span of 8.90 m; any resemblance to the Grumman X-29A is purely coincidental! For the purposes of the present experimental study a one fourteenth dynamically scaled wind tunnel model was designed and built as described by Heydari[7]. The wind tunnel model is shown in Figure 1 and incorporates servo driven foreplane, ailerons and rudder and a central gimbal system for attachment to the wind tunnel rig. The model is highly modular and includes facilities for mass, inertia, C.G. position and stability margin adjustment.

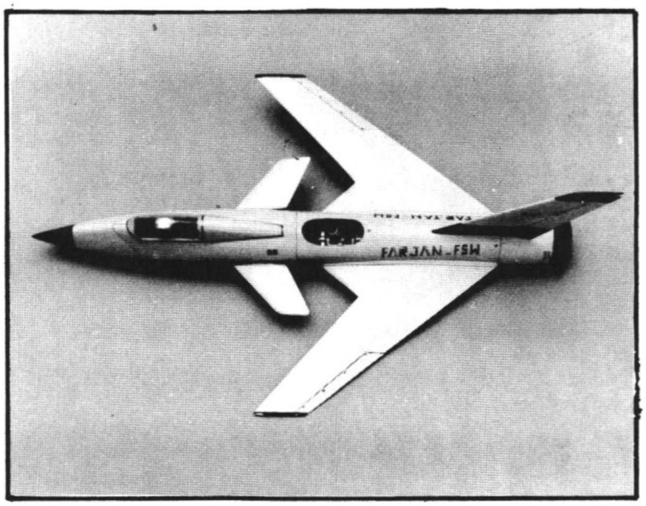

Figure 1. The FSW Aircraft Model

THE EXPERIMENTAL FACILITY

Equipment description

The experimental facility was intended from the outset to be a small scale low cost facility, initially studied by Kumar[1] and subsequently designed and developed by Malik[2]. The equipment comprises a low speed wind tunnel, model suspension system, electronic control unit, recording equipment and interface to a digital computer. A functional block diagram of the facility is shown on Figure 2.

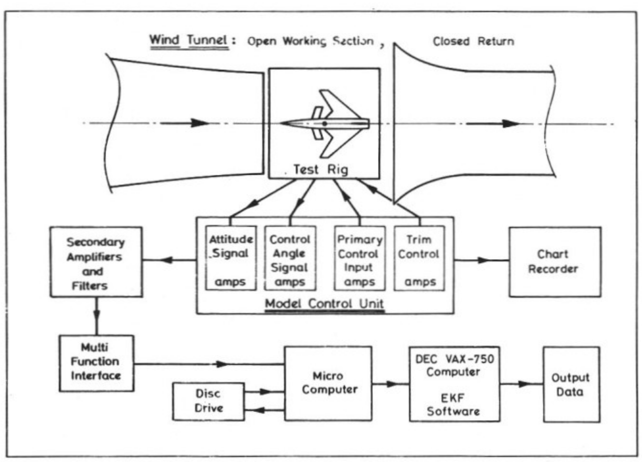

Figure 2. The Experimental Facility

The entire facility is limited by the wind tunnel which is an open working section closed return type in which the maximum velocity is approximately 40 m/sec. The suspension system framework is placed in the working section and the model is constrained to a fixed vertical rod supported by the framework. The model incorporates a gimbal which permits it to roll, pitch and yaw relative to the vertical rod and to slide vertically along the rod. The model is shown attached to the suspension system in Figure 3. The analogue electronic control unit is connected to the model and provides the means for controlling the model and for the acquisition of control and response signal data for recording. Signals available from the equipment comprise control surface angles, roll, pitch and yaw attitude relative to rig datum and model position on the vertical rod. A paper by Cook and Malik[3] provides a summary description of the equipment, the dynamic scaling requirements and a brief review of its performance capabilities.

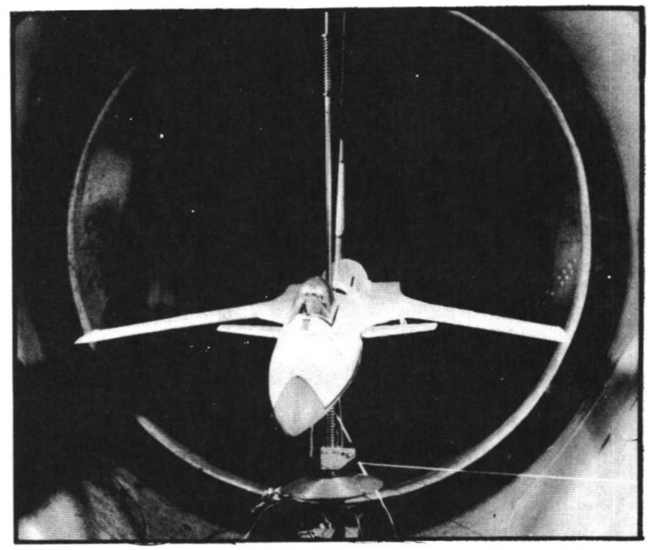

Figure 3. FSW Aircraft Model on Test Rig

Model equations of motion

The small perturbation equations of motion are described with respect to a wind axis system fixed in the model such that the origin of the axes, the C.G. of the model and the centre of the suspension gimbal are all coincident. The axis system (oxyz) and the four degrees of freedom of the model w, Φ, Θ and ψ are shown in Figure 4.

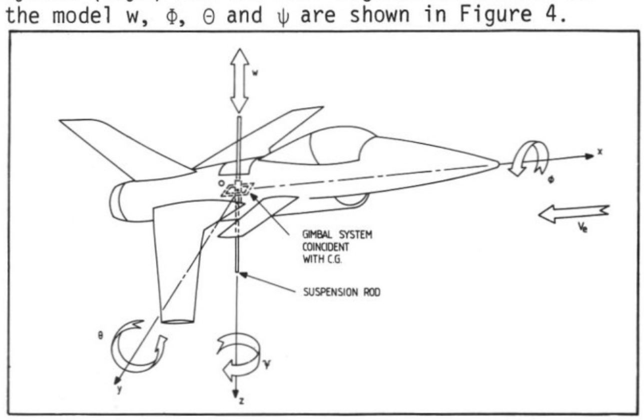

Figure 4. FSW Model Degrees of Freedom

Further, the fore and aft axis ox is parallel to the wind tunnel axis in the undisturbed state. In state space form the equations of motion are;

Longitudinal

$$\begin{bmatrix} \dot{w} \\ \dot{q} \\ \dot{\Theta} \end{bmatrix} = \begin{bmatrix} Z_w & (Z_q + U_e) & 0 \\ M_w & M_q & 0 \\ 0 & 1 & 0 \end{bmatrix} \begin{bmatrix} w \\ q \\ \Theta \end{bmatrix} + \begin{bmatrix} Z_\eta \\ M_\eta \\ 0 \end{bmatrix} \eta \qquad \text{(i)}$$

and,

$$\begin{bmatrix} w \\ q \\ \Theta \end{bmatrix} = \begin{bmatrix} 1 & 0 & 0 \\ 0 & 1 & 0 \\ 0 & 0 & 1 \end{bmatrix} \begin{bmatrix} w \\ q \\ \Theta \end{bmatrix} + \begin{bmatrix} 0 \\ 0 \\ 0 \end{bmatrix} \eta \qquad \text{(ii)}$$

Lateral

$$\begin{bmatrix} \dot{v} \\ \dot{p} \\ \dot{r} \\ \dot{\Phi} \end{bmatrix} = \begin{bmatrix} 0 & 0 & -U_e & 0 \\ L_v & L_p & L_r & 0 \\ N_v & N_p & N_r & 0 \\ 0 & 1 & 0 & 0 \end{bmatrix} \begin{bmatrix} v \\ p \\ r \\ \Phi \end{bmatrix} + \begin{bmatrix} 0 & 0 \\ L_\xi & L_\zeta \\ N_\xi & N_\zeta \\ 0 & 0 \end{bmatrix} \begin{bmatrix} \xi \\ \zeta \end{bmatrix} \qquad \text{(iii)}$$

and,

$$\begin{bmatrix} v \\ p \\ r \\ \Phi \end{bmatrix} = \begin{bmatrix} 1 & 0 & 0 & 0 \\ 0 & 1 & 0 & 0 \\ 0 & 0 & 1 & 0 \\ 0 & 0 & 0 & 1 \end{bmatrix} \begin{bmatrix} v \\ p \\ r \\ \Phi \end{bmatrix} + \begin{bmatrix} 0 & 0 \\ 0 & 0 \\ 0 & 0 \\ 0 & 0 \end{bmatrix} \begin{bmatrix} \xi \\ \zeta \end{bmatrix} \qquad \text{(iv)}$$

The aerodynamic stability and control derivatives are in the usual dimensional concise form.

THE KALMAN FILTER ESTIMATOR

For the purposes of estimating the aerodynamic stability and control derivatives of the model from a computer based analysis of recorded input and output response data a Kalman filter technique was used. The usual difficulties of providing an initial guess at the derivatives and the definitions of process and measurement noise were relatively easily overcome since, calculated estimates of the derivatives had been made earlier in the programme and bandwidth limited white noise was considered adequate for the simple system in question. A full description of the development of the Kalman filter is given by Heydari(7) and a brief summary follows.

System equations

Assuming the sytem of interest can be described by a set of simultaneous linear differential equations then, in state space form these may be written,

$$\dot{\underline{x}}(t) = A\,\underline{x}(t) + B\,\underline{u}(t) \qquad \text{(v)}$$

and,

$$\underline{y}(t) = C\,\underline{x}(t) + D\,\underline{u}(t) \qquad \text{(vi)}$$

where equation (v) is the state equation and equation (vi) is the output equation. When the system is discrete and noise is present the corresponding equations can be derived from the continuous equations,

$$\underline{x}(n+1) = \Phi(n)\,\underline{x}(n) + \psi(n)\,\underline{u}(n) + \Theta(n)\,\underline{w}(n) \qquad \text{(vii)}$$

and,

$$\underline{y}(n) = C(n)\,\underline{x}(n) + D(n)\,\underline{u}(n) + \underline{v}(n) \qquad \text{(viii)}$$

where $\underline{w}(n)$ and $\underline{v}(n)$ are the process and measurement noise vectors respectively, $\Phi(n)$ is the discrete state transition matrix, $\psi(n)$ is the discrete input matrix and $\Theta(n)$ is the process noise matrix.

The discrete Kalman filter

Provided that the system described by equations (v) and (vi) is observable then a Kalman filter can be used to estimate its states. The discrete Kalman filter estimates corresponding to equations (vii) and (viii) are given by,

$$\hat{\underline{x}}(n+1) = \Phi(n)\,\hat{\underline{x}}(n) + \psi(n)\,\underline{u}(n) + P(n)[\underline{y}(n) - C(n)\,\hat{\underline{x}}(n) - D(n)\underline{u}(n)] \qquad \text{(ix)}$$

and

$$\hat{\underline{y}}(n) = \hat{\underline{x}}(n) \qquad \text{(x)}$$

where (^) indicates an estimated value. A measure of the state estimation "error" is given by the error covariance matrix,

$$G(n) = E[(\underline{x}(n) - \hat{\underline{x}}(n))(\underline{x}(n) - \hat{\underline{x}}(n))^T] \qquad \text{(xi)}$$

The Kalman filter is optimal in that the gain matrix P(n) is calculated to minimise the state estimation error by minimising the trace of G(n). The optimal value of P(n) is given by,

$$P(n) = \Phi(n)G(n)C(n)^T[C(n)G(n)C(n)^T + R]^{-1} \qquad \text{(xii)}$$

and the value of the error covariance matrix at the (n+1)th iteration is given by,

$$G(n+1) = [\Phi(n) - P(n)C(n)]G(n)\Phi(n)^T + \Theta(n)Q\Theta(n)^T \qquad \text{(xiii)}$$

where Q and R are the process and measurement noise covariance matrices respectively.

Evaluation of the Kalman filter requires that, given the appropriate initial conditions, equations (xii), (ix) and (xiii) are calculated for $n = 1,2,3 \ldots\ldots\infty$.

The split Kalman filter

When the period between data sample updates is large relative to the computational iteration period then the estimation accuracy may deteriorate. To overcome this difficulty a split Kalman filter is used in which two different sets of estimation equations are computed according as the time step is also a measurement sample update or just simply a time iteration between sample updates.

Measurement update filter equations

$$J(n) = G^-(n)C(n)^T[R + C(n)G^-(n)C(n)^T]^{-1} \qquad \text{(xiv)}$$

$$\hat{\underline{x}}^+(n) = \hat{\underline{x}}^-(n) + J(n)[\underline{y}(n) - C(n)\hat{\underline{x}}^-(n) - D(n)\underline{u}(n)] \qquad \text{(xv)}$$

$$G^+(n) = [I - J(n)C(n)]G^-(n) \qquad \text{(xvi)}$$

Time update filter equations

$$\hat{\underline{x}}^-(n+1) = \Phi(n)\hat{\underline{x}}^+(n) + \psi(n)\,\underline{u}(n) \qquad \text{(xvii)}$$

$$G^-(n+1) = \Phi(n)G^+(n)\Phi(n)^T + \Theta(n)Q\Theta(n)^T \qquad \text{(xviii)}$$

The output equation is given by,

$$\hat{\underline{y}}(n) = \hat{\underline{x}}^{+}(n) \qquad \text{(xix)}$$

where the superscript (-) refers to the value of the estimate in the previous iteration interval and the superscript (+) refers to the value of the estimate in the next iteration interval. The split Kalman filter gain matrix J(n) is related to the gain matrix P(n) by the state transition matrix $\Phi(n)$ viz,

$$P(n) = \Phi(n)J(n) \qquad \text{(xx)}$$

The extended Kalman filter

When the coefficients of the state transition matrix and the input matrix are unknown then the estimation problem becomes non-linear as estimates of these coefficients also have to be found. In this special case the system equations (vii) and (viii) may be redefined,

$$\underline{x}(n+1) = \underline{f}[\underline{x}(n),\underline{u}(n)] + E[\underline{x}(n)]\underline{w}(n) \qquad \text{(xxi)}$$

and,

$$\underline{y}(n) = \underline{g}[\underline{x}(n),\underline{u}(n)] + \underline{v}(n) \qquad \text{(xxii)}$$

where $\underline{f}$ is the state transition function matrix, $\underline{g}$ is the output function matrix and E is the process noise matrix.

The split Kalman filter estimator may be extended to cope with this system, the estimation equations (xv), (xvii) and (xix) then become,

$$\hat{\underline{x}}^{+}(n) = \hat{\underline{x}}^{-}(n) + J(n)[\underline{y}(n) - \underline{g}\{\hat{\underline{x}}^{-}(n), \underline{u}(n)\}] \qquad \text{(xxiii)}$$

$$\hat{\underline{x}}^{-}(n+1) = \underline{f}[\hat{\underline{x}}^{+}(n), \underline{u}(n)] \qquad \text{(xxiv)}$$

and,

$$\hat{\underline{y}}(n) = \hat{\underline{x}}^{+}(n) \qquad \text{(xxv)}$$

After some further analysis it may be shown that the state transition matrix is given by,

$$\Phi(n) = \left[\frac{\partial \underline{f}[\underline{x}(n), \underline{u}(n)]}{\partial \underline{x}(n)}\right]_{\underline{x}(n) = \underline{x}^{+}(n)} \qquad \text{(xxvi)}$$

the output matrix is given by,

$$C(n) = \left[\frac{\partial \underline{g}[\underline{x}(n), \underline{u}(n)]}{\partial \underline{x}(n)}\right]_{\underline{x}(n) = \underline{x}^{-}(n)} \qquad \text{(xxvii)}$$

and the process noise matrix is given by,

$$\Theta(n) = E[\hat{x}^{+}(n)] \qquad \text{(xxviii)}$$

The matrices J(n), $G^{-}(n+1)$ and $G^{+}(n)$ are as defined by equations (xiv), xviii) and (xvi) respectively.

The Kalman filter implementation

A program was written to implement the extended Kalman filter estimator on a DEC VAX 11/750 computer. A flow chart describing the computational steps in the estimation process is shown on Figure 5. Program initialisation requires that

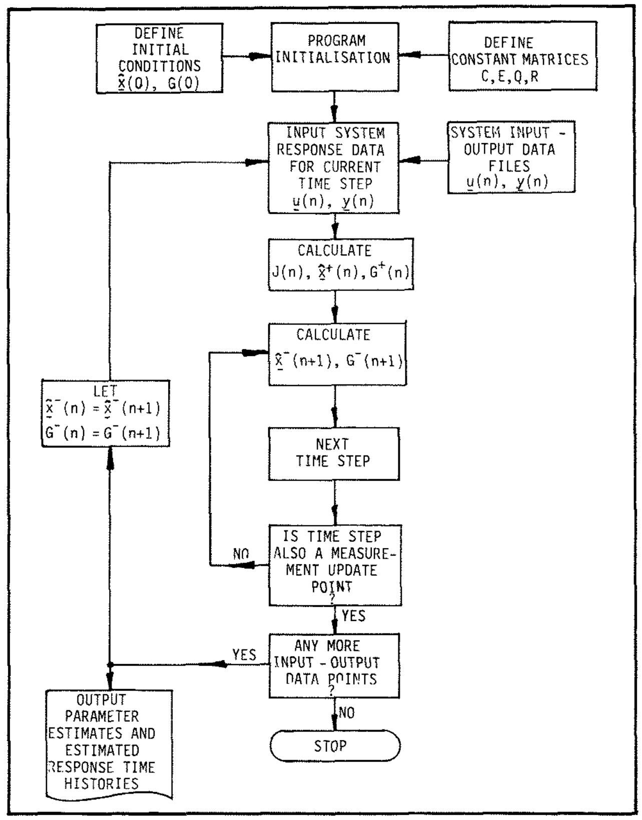

Figure 5. Parameter Estimation Program Flow Diagram.

initial estimates of the state variables and the system parameters are made together with an estimate of the initial value of the error covariance matrix G. The computational process is simplified as some system matrices are constant. In particular the output matrix C and the noise matrices E, Q and R are constant whereas, the direct matrix D is zero; all are defined numerically at initialisation. Digital input and output response records obtained from the wind tunnel model are stored in data files and are accessed during program execution. The computational steps in the program are self evident and the functional expressions corresponding to the various stages in the calculation are defined by the appropriate equations above.

APPLICATION TO THE DYNAMIC MODEL

As an example consider the application of the extended Kalman filter estimation algorithm to the longitudinal equations of motion of the FSW aircraft model as defined by equations (i) and (ii). An essential prerequisite to program execution is the proper definition of the system, filter, noise and error matrices as well as some initial conditions.

Kalman filter equations

The real time equivalent of the system equations (xxi) and (xxii) may be written,

$$\begin{bmatrix}\dot{w}\\ \dot{q}\\ \dot{\Theta}\\ \dot{Z}_w\\ \dot{M}_w\\ \dot{M}_q\\ \dot{Z}_\eta\\ \dot{M}_\eta\end{bmatrix} = \begin{bmatrix}Z_w w & U_e q & Z_\eta \eta\\ M_w w & M_q q & M_\eta \eta\\ 0 & q & 0\\ 0 & 0 & 0\\ 0 & 0 & 0\\ 0 & 0 & 0\\ 0 & 0 & 0\\ 0 & 0 & 0\end{bmatrix} + \begin{bmatrix}0&0&0&0&0\\0&0&0&0&0\\0&0&0&0&0\\1&0&0&0&0\\0&1&0&0&0\\0&0&1&0&0\\0&0&0&1&0\\0&0&0&0&1\end{bmatrix}\begin{bmatrix}w_1\\w_2\\w_3\\w_4\\w_5\end{bmatrix} \qquad \text{(xxix)}$$

and,

$$\begin{bmatrix}w\\q\\\Theta\end{bmatrix} = \begin{bmatrix}1&0&0&0&0&0&0&0\\0&1&0&0&0&0&0&0\\0&0&1&0&0&0&0&0\end{bmatrix}\begin{bmatrix}w\\q\\\Theta\\Z_w\\M_w\\M_q\\Z_\eta\\M_\eta\end{bmatrix} + \begin{bmatrix}v_1\\v_2\\v_3\end{bmatrix} \qquad \text{(xxx)}$$

Consequently the matrices $f[\underline{x}(n),\underline{u}(n)]$, $g[\underline{x}(n),\underline{u}(n)]$ and $E[\underline{x}(n)]$ are defined. The derivative Z_q is omitted as it is assumed $Z_q \ll U_e$ and it is noted that the direct matrix D is zero. The column vectors in equation (xxix) and (xxx) are also readily defined in terms of system state variables, the parameters to be identified and noise components. These equations can be converted into discrete form with the aid of the simple forward difference algorithm,

$$\dot{\underline{x}}(t) \equiv \left[\frac{\underline{x}(n+1) - \underline{x}(n)}{h}\right] \qquad \text{(xxxi)}$$

State transition matrix

The discrete state transition matrix $\Phi(n)$ follows as given by equation (xxvi) and may be derived,

$$\Phi(n) = \begin{bmatrix}(1+hZ_w) & hU_e & 0 & hw & 0 & 0 & h\eta & 0\\ hM_w & (1+hM_q) & 0 & 0 & hw & hq & 0 & h\eta\\ 0&0&1&0&0&0&0&0\\ 0&0&0&1&0&0&0&0\\ 0&0&0&0&1&0&0&0\\ 0&0&0&0&0&1&0&0\\ 0&0&0&0&0&0&1&0\\ 0&0&0&0&0&0&0&1\end{bmatrix} \qquad \text{(xxxii)}$$

Initial state estimates

Initial estimates for the Kalman filter states comprising the system state variables and the stability derivatives are given in Table 1. Also quoted are estimated maximum values and estimates of r.m.s. error associated with each state variable. The maximum values of the system state variables are based on observation and the errors are assumed to be 1% of the maximum values. The initial and maximum values of the stability derivatives are based on calculation and their errors are assumed to be 10% of the maximum values.

TABLE 1 INITIAL STATE ESTIMATES

FILTER STATES	INITIAL VALUE	MAXIMUM VALUE	ε r.m.s. ERROR	UNITS
w	0	4.0	0.04	m/s
q	0	1.0	0.01	rad/s
Θ	0	0.4	0.004	rad
Z_w	-2.0	-2.0	-0.2	1/s
M_w	-0.2	-0.2	-0.02	$\frac{1}{m.s.}$
M_q	-0.8	-0.8	-0.08	$\frac{1}{s}$
Z_η	-10.0	-10.0	-1.0	$\frac{m}{s^2.rad}$
M_η	40.0	40.0	-4.0	$\frac{1}{s^2}$

Error covariance matrix

The error covariance matrix G(n) is given by equation (xi) and is an 8 x 8 diagonal matrix. If the non-zero diagonal elements are denoted g_{ii} then the initial estimate of this matrix G(0) is given by,

$$g_{ii} = \varepsilon_i^2\ , \quad i = 1,2,3 \ldots 8.$$

where ε_1 is the r.m.s. error in w, ε_2 is the r.m.s. error in q and so on.

Noise covariance matrices

As defined in this application the process and measurement noise covariance matrices Q and R are constant diagonal matrices with non-zero elements q_{ii} and r_{ii} respectively. This follows from the assumption that the process and measurement noise vectors are uncorrelated with each other and with the initial system states. The noise models were assumed to be bandwidth limited white noise and after substantial analysis, as described by Heydari(7), it may be shown that,

$$q_{ii} = \frac{2nh}{\pi}\,\varepsilon^2_{(i+3)} \qquad i = 1,2,\ldots 5.$$

and,

$$r_{ii} = \frac{2nh}{\pi}\,\varepsilon_i^2, \qquad i = 1,2,3.$$

where, as before ε_1, ε_2, ε_3 are the r.m.s. errors in the measured parameters w,q,Θ and, ε_4 to ε_8 are the r.m.s. errors in the estimated parameters Z_w, M_w, etc, as given in Table 1. In this application the number of iterations n between samples is 100 and the iteration period is 0.01 seconds.

Output matrix

The output matrix C(n) is defined by equation (xxvii). However, by reference to equation (xxx) it is evident that this matrix is a simple constant matrix,

$$C = \begin{bmatrix} 1 & 0 & 0 & 0 & 0 & 0 & 0 & 0 \\ 0 & 1 & 0 & 0 & 0 & 0 & 0 & 0 \\ 0 & 0 & 1 & 0 & 0 & 0 & 0 & 0 \end{bmatrix}$$

Process noise matrix

In transforming equations (xxix) and (xxx) to the discrete form it may be shown that the process noise matrix is also a constant matrix dependent only on the iteration interval h viz,

$$E = \begin{bmatrix} 0 & 0 & 0 & 0 & 0 \\ 0 & 0 & 0 & 0 & 0 \\ 0 & 0 & 0 & 0 & 0 \\ h & 0 & 0 & 0 & 0 \\ 0 & h & 0 & 0 & 0 \\ 0 & 0 & h & 0 & 0 \\ 0 & 0 & 0 & h & 0 \\ 0 & 0 & 0 & 0 & h \end{bmatrix}$$

Rate derivation

Response measurements from the dynamic model include pitch attitude Θ and vertical position on the support rod. As the rates of change of these two variables $\dot{\Theta}$,(q) and w were required to complete the system state variable complement they had to be obtained by differentiation. Both analogue and numerical differentiation were considered unsuitable as the noise content of the derived states was unacceptable. The problem was overcome by fitting a 21st order Chebyshev polynomial to the attitude data and then differentiating the polynomial analytically to obtain the corresponding rate data.

ESTIMATOR PERFORMANCE

The parameter estimation program was developed and validated with the aid of a computer simulation of the same four degrees of freedom aircraft model as used in the Kalman filter. Input and output response "measurements" were obtained from the simulation which was programmed in the Advanced Continuous Simulation Language (ACSL) and incorporated known arbitrary values of the derivatives to be estimated. It was not entirely surprising that the parameter estimates thus obtained were a very good match with the known values. The parameter identification software was validated with a number of experiments of this nature prior to its used with data obtained from the wind tunnel model.

No significant problems were encountered with the stability of the estimation algorithm the derivative estimates converging to steady values in well under 500 iterations and, in many instances in around 200 iterations. The number of iterations required to achieve convergence and the nature of the convergence were found to be quite dependent on the type of input used to disturb the simulation model. A comparison of some typical stability derivative estimates with the actual values are included in Table 2. Longitudinal derivatives were estimated from responses to a dipole or sinusoidal elevator input and in either case it is clear that quite acceptable results were obtained, the dipole input producing marginally better results. For the lateral example shown the derivatives were estimated from the response to a dipole aileron input and it is clear that the results are very good. However, it should be borne in mind that no noise was present in the data samples used for this exercise.

TABLE 2. COMPARISON OF ACTUAL WITH ESTIMATED PARAMETERS

STABILITY DERIVATIVE	ACTUAL VALUE	ESTIMATED VALUE	
		DIPOLE INPUT	SINUSOIDAL INPUT
Z_w	-2.0	-2.0	-3.0
M_w	-0.2	-0.2	-0.5
M_q	-0.8	-0.7	-1.1
Z_η	-10.0	-15.0	-16.0
M_η	40.0	45.0	32.0
L_v	-20.0	-20.0	
L_p	-5.0	-5.0	
L_r	1.5	1.0	
N_v	15.0	15.0	
N_p	1.5	1.5	
N_r	-5.0	-5.0	
L_ξ	50.0	50.0	
N_ξ	-6.0	-4.5	

RESULTS

The FSW aircraft model is only capable of simulating the short period modes of motion as it only has four degrees of freedom. However, it has been shown in earlier work(3) that the longitudinal short period pitching oscillation and the roll subsidence mode are reproduced well whereas, the dutch roll mode is generally less accurate. It was therefore expected that the parameter identification program would produce the best estimates of those derivatives which are dominant in determining the characteristics of the short period modes and indeed, as far as could be ascertained this was borne out by the results.

In all experiments with the unaugmented model, motion responses were obtained by disturbing the model from trimmed flight by the application of the appropriate control surface input. Some practical difficulties were encountered as a result of unsteady flow near the edge of the wind tunnel jet, flow resonance at lower speeds, marginal model stability and sensitive model controls all of which combined to make trimming and response testing very difficult at some flight conditions.

Longitudinal derivative estimates

The longitudinal response to an impulse applied to the foreplane was recorded for four speeds and two C.G. positions. Estimates of the dimensionless longitudinal derivatives were made from these responses and the results are shown in Table 3. Each experiment was repeated a number of times and the mean values are quoted in the table. The C.G. positions were ahead of the mean aerodynamic chord, hence the negative value, and the speeds are the full scale equivalent values at sea level.

TABLE 3. ESTIMATED LONGITUDINAL DERIVATIVES

	C.G. at -18.5% $\bar{\bar{c}}$		C.G. at -16.1% $\bar{\bar{c}}$	
	V_e = 98m/sec	V_e = 109m/sec	V_e = 95m/sec	V_e = 102m/sec
Z_w	-8.0	-9.6	-9.2	-12.0
Z_q	-328.2	-314.4	-338.7	-338.7
M_w	3.3	3.4	3.9	4.8
M_q	-4.0	-6.9	-2.8	-6.2
Z_η	-6.1	-9.2	—	-13.5
M_η	1.9	2.3	—	3.0

Owing to "tunnel noise" difficulties as mentioned above it was found impossibly difficult to obtain sensible estimates for Z_η and M_η at 95 m/sec and hence these are omitted from the table. Otherwise the values of the derivatives were more or less consistent with theoretical estimates with the exception of Z_q. As its value is abnormally large it was essential to include Z_q in the model equations of motion in order to obtain an acceptable estimate of the other parameters. After some investigation Z_q was found to be largely due to the non-linear friction effects in the vertical motion of the model and, as such, could not be satisfactorily modelled separately. The positive value of M_w indicated the model to be unstable which was confirmed by calculations of stability margin. That the model could be trimmed at all resulted from the non-linear C_m-α characteristic, the model being trimmed initially at a marginally stable incidence. Owing to the relative simplicity of the model these more significant non-linear effects were not separately identified.

A typical short period mode response is shown on Figure 6 where the actual and estimated transients for the same input data are compared. Clearly the estimate is in reasonable agreement with the actual response implying that the dominant derivatives were adequately estimated. To obtain further confidence in these results a four degree of freedom computer simulation of the FSW model aircraft was written in the ACSL which incorporated the estimated stability derivatives. The response to a foreplane impulse input is shown on Figure 7 and again, reasonable agreement between this response and those shown on Figure 6 is evident although the simulation model appears to have higher damping. It was therefore concluded that the longitudinal derivative estimates were reasonable for the FSW model but that their application to full scale free flight conditions should be undertaken with caution.

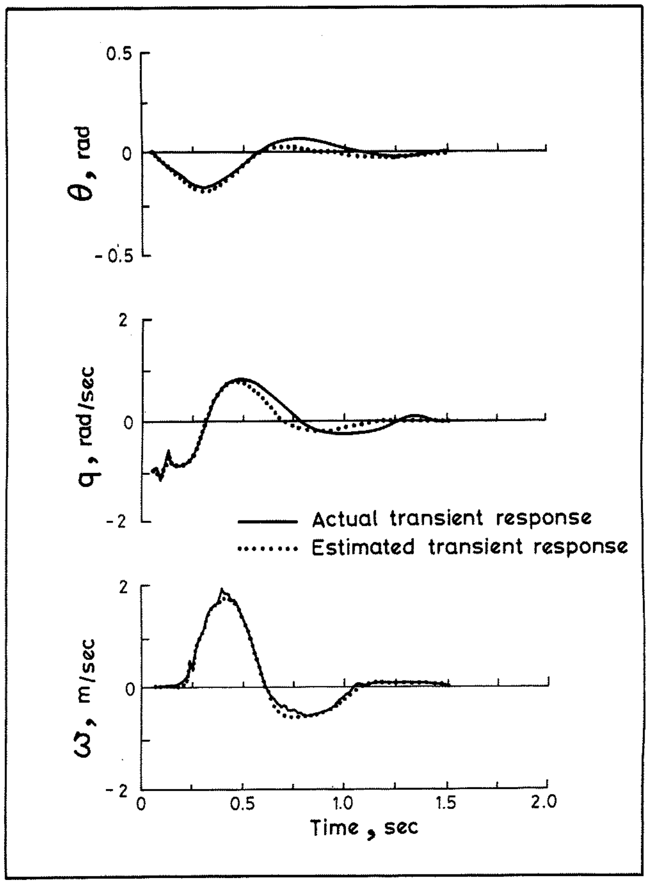

Figure 6. Typical Longitudinal Short Period Mode Responses.

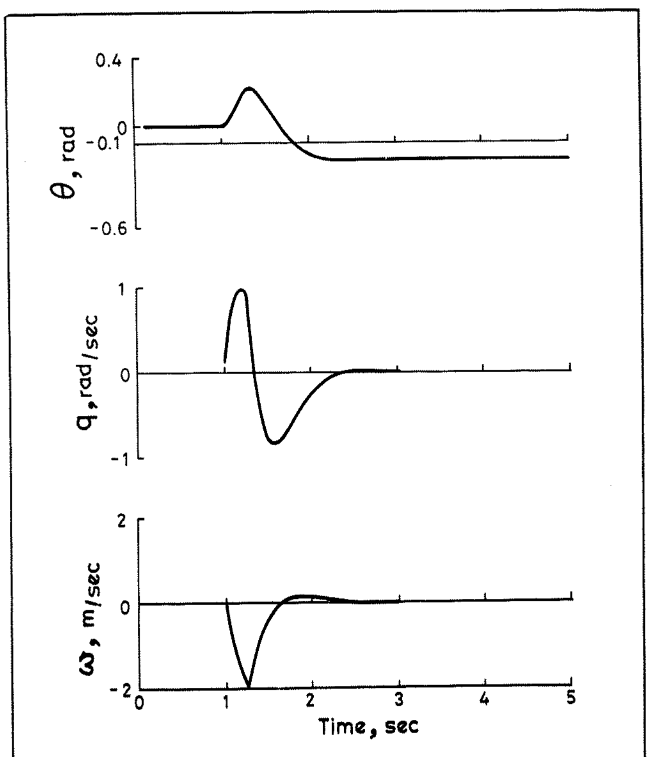

Figure 7. Typical Simulated Longitudinal Short Period Mode Responses.

Lateral derivative estimates

The lateral response to an impulse applied to the rudder was recorded for four speeds and two C.G. positions. It was not possible to obtain response records for any aileron input as the model has a marginally unstable spiral mode and the normally slow roll divergence was severely aggravated by the unsteady tunnel flow characteristics mentioned above. Thus for the purposes of the present exercise the dutch roll mode was excited by the application of a small amplitude rudder impulse to the nominally trimmed model. Provided the experiments were carefully set up and provided that the period of observation was relatively short satisfactory responses could be obtained in most instances. That the model could be trimmed at all was attributed to the static friction in the mounting gimbal system which was not incorporated explicitly in the estimation model. In view of the fact that the parameter estimation was based on an analysis of dutch roll mode responses it was anticipated that those derivatives which play a dominant role in characterizing the mode would be estimated with the highest degree of confidence. Estimates of the dimensionless lateral derivatives thus obtained are contained in Table 4. As in the longitudinal case the C.G. positions quoted are ahead of the mean aerodynmamic chord and the speeds refer to the full scale equivalent values at sea level.

TABLE 4. ESTIMATED LATERAL DERIVATIVES

	C.G. at -18.5% $\bar{\bar{c}}$				C.G. at -16.1% $\bar{\bar{c}}$
	V_e = 98 m/sec	V_e = 105 m/sec	V_e = 113 m/sec	V_e = 120 m/sec	V_e = 98 m/sec
L_v	0.09	0.02	0.08	0.04	0.03
L_p	-1.72	-0.27	-0.56	-0.92	-1.15
L_r	-0.29	-0.16	-0.12	-0.11	-0.46
N_v	0.55	0.20	0.36	0.27	0.60
N_p	22.03	23.67	23.62	22.88	-1.69
N_r	-7.63	-5.68	-5.90	-6.24	-6.78
L_ζ	0.20	0.18	0.17	0.17	0.17
N_ζ	2.26	2.12	1.62	1.30	3.17

Again, the derivative estimates quoted are the mean values obtained from a number of repeated experiments and it can be seen that acceptably consistent estimates were obtained with the possible exception of N_p. The value for L_v is positive as might be expected in an aircraft with an unstable spiral mode and is consistent with the F.S.W. geometry. Although the reason for the uncharacteristically large value of N_p has not been conclusively identified a number of contributory factors have been recognised. These factors may of course influence the estimates of the other derivatives as well.

It has become apparent that the static and dynamic friction effects of the model support system have a significant influence on the dynamic behaviour of the aircraft and as these effects are not separately modelled in the estimation program so their influence is implicit in the derivative estimates. In view of the complexity of these friction contributions, to have separated them out in the mathematical models would have been beyond the scope of the present work.

In defining the extended Kalman filter as an optimal filter it was assumed that there is no correlation between measured or derived system state variables. However, in the lateral motions of the aircraft model there is very pronounced coupling between rolling and yawing motion. The filter was therefore applied to a condition for which it was non-optimum. As a result it was found that the output estimates were dependent on the proper choice of covariance matrices Q and R. In particular it was found difficult to define the covariance matrix R adequately. It was possible to establish a very good match between recorded and estimated transient responses which seemed relatively independent of the choice of the measurement noise covariance matrix R. However, in order to obtain convergent derivative estimates the choice of R was critical and, depending on the choice of R, a trade-off in relative values of the estimated roll-yaw coupling derivatives L_r and N_p was possible. These difficulties were resolved by basing the estimates of the matrices Q and R on accrued evidence until reasonable derivative estimates were obtained and, it is suspected that N_p was a casualty in this process.

DISCUSSION AND CONCLUSIONS

As part of an extensive programme of research into the stability and control characteristics and the stability augmentation requirements of a FSW combat aircraft an exercise was undertaken to estimate the aerodynamic stability derivatives with the aid of a dynamic wind tunnel model. A one fourteenth scale model of the aircraft design was built and flown in a low speed wind tunnel whilst supported by a purpose built test rig. Transient responses to defined control inputs were recorded and analysed using a parameter estimation procedure developed for the purpose and from which estimates of some stability derivatives were obtained. As the model suspension system permitted four degrees of freedom it was only possible to reproduce the short period modes of motion and consequently, to estimate only those derivatives appropriate to the reduced model.

The parameter estimation was achieved with a computer program written to utilise an extended Kalman filter algorithm as, of the techniques available, it was the most convenient for a number of reasons. In particular a considerable amount of information was already available concerning the practical implementation of the technique. The application of a Kalman filter estimator to the experimental facility was relatively straight forward since the system model was simple, the experimental conditions were near ideal and a significant amount of numerical data for the model was already available. An additional consideration in choosing to use a Kalman filter was its applicability to real time estimation, although not used in this way further developments in this respect were not ruled out. The main problems encountered were a result of using a not entirely representative system model in the Kalman filter. The system model contained two major shortcomings; firstly, static and dynamic friction effects in the model suspension system were found to be significant and were not modelled separately and, secondly, in defining the Kalman filter it was assumed that the system state variables were uncorrelated which was not properly representative since motion coupling was present. Once these limitations were understood their influence was minimised by developing an appropriate experimental procedure but, as these effects could not be entirely eliminated some care is necessary in the interpretation of the derivative estimates. In any future development of the facility it would obviously be sensible to attempt a further reduction in model suspension system friction and to modify the Kalman filter system model to incorporate these frictional contributions explicitly. Additionally, provision should be made in the filter algorithm for motion coupling effects and the corresponding correlation between the variables involved although this might be very difficult to implement in practice.

The aerodynamic stability derivatives were estimated from the longitudinal short period mode and the lateral dutch roll mode transient responses. For practical reasons it was not possible to obtain usable roll subsidence mode transient responses. Available evidence suggests that the derivative estimates are numerically reasonable and correlate well with known aircraft characteristics. However, caution must be applied in the interpretation of the derivative values since some derivatives are better represented than others in the short period mode responses and, in every case, some contribution from the model support system friction is implied. In this respect it was discovered that the derivative Z_q is grossly distorted by friction in the vertical motion and the derivative N_p is believed to be too large as a result of friction in rolling and yawing motion in combination with inadequate provision for roll-yaw motion coupling in the estimation model. Thus, it has been demonstrated that, provided due allowance is made for its shortcomings and limitations then, the experimental facility described can provide useful stability and control data for unconventional aircraft configurations with a fair degree of confidence.

REFERENCES

1. Kumar, H. "A preliminary study into the design of a free flight wind tunnel model for demonstrating the dynamic characteristics of aircraft." College of Aeronautics M.Sc. thesis 1980.

2. Malik, I.A. "The design, development and evaluation of an active control aircraft model wind tunnel facility." College of Aeronautics Ph.D. thesis, 1982.

3. Cook, M.V. and Malik, I.A. "The dynamic simulation of aircraft using actively controlled models in a wind tunnel." Proc. UKSC Conference on Computer Simulation, Butterworths, 1984.

4. Cook, M.V. and O'Riordan, S.J.P. "A technique for optimising the aerodynamic design of a generalised combat aircraft with forward swept wings for the purposes of stability and control investigation." College of Aeronautics Report 8325, January 1984.

5. O'Riordan, S.J.P. "Automated design optimisation of a forward swept wing fighter for stability studies." College of Aeronautics M.Sc. thesis, 1984.

6. Heydari, F. and Cook, M.V. "The development of a dynamic model of a generalised combat aircraft with forward swept wings for the identification of stability and control characteristics." College of Aeronautics Report 8433, October 1984.

7. Heydari, F. "On the estimation of stability and control characteristics of a generalised forward swept wing aircraft." College of Aeronautics PhD thesis, to be published 1986.

ACKNOWLEDGEMENT

The programme of work described was sponsored by the Ministry of Defence (Procurement Executive) and the authors gratefully acknowledge the support and encouragement provided by the technical monitor, Dr A J Ross of the Royal Aircraft Establishment, Farnborough.